International Science and Technology Journal
المجلة الدولية للعلوم والتقنية
Volume 37 العدد
Part 1 المجلد
المجلة الدولية للعلوم والتقنية
International Science and Technology Journal
ISTJ

http://www.doi.org/10.62341/smay0803

Received	**2025/08/05**	**تم استلام الورقة العلمية في**
Accepted	**2025/08/29**	**تم قبول الورقة العلمية في**
Published	**2025/08/30**	**تم نشر الورقة العلمية في**

Comparative Evaluation of Photovoltaic Array Reconfiguration Techniques

Samer Al-refai[1], Mohamed Y B Husain[2*]

[1] Department of Electric and Electronic, Higher institute of science and Technology, Tobruk, Libya

[2] Department of physics, Faculty of science, Tobruk University, Tobruk, Libya
Correspondence Author: * Mohamed.husain@tu.edu.ly

Abstract:

The purpose of this study is to assess methods for reconfiguring solar arrays to lessen the adverse effects of partial shade. MATLAB was used to examine and simulate a number of reconfiguration and connecting techniques. According to the findings, reconfiguration strategies including dynamic electrical schemes and adaptive banking greatly increase PV system efficiency when compared to traditional approaches using Matlab/Simulink. Moreover, combining these strategies with MPPT algorithms enhances system performance in conditions involving partial shading. In order to guarantee greater stability and efficiency, the study suggests implementing reconfiguration techniques in PV system design. For future work, it is suggested to experimentally validate these algorithms on real PV systems and assess their integration with microgrids under diverse operating environments.

Keywords: MPPT, partial shading, photovoltaic cells, solar energy, reconfiguration.

International Science and Technology Journal
المجلة الدولية للعلوم والتقنية
Volume 37 العدد
Part 1 المجلد
المجلة الدولية للعلوم والتقنية
International Science and Technology Journal
ISTJ
http://www.doi.org/10.62341/smay0803

التقييم المقارن لتقنيات إعادة تشكيل مصفوفات الخلايا الكهروضوئية

سامر الرفاعي [1] , محمد يونس بكار حسين [2*]

قسم الكهرباء والالكترونات، المعهد العالي للعلوم والتقنية، طبرق، ليبيا[1]
قسم الفيزياء، كلية العلوم، جامعة طبرق، طبرق، ليبيا[2]
* Mohamed.husain@tu.edu.ly

الملخص

يهدف هذا البحث إلى تقييم تقنيات إعادة تشكيل مصفوفات الخلايا الكهروضوئية للتقليل من الآثار السلبية للتظليل الجزئي. تم دراسة ومقارنة عدد من طرق التوصيل وإعادة التشكيل باستخدام محاكاة في برنامج **MATLAB**. أظهرت النتائج أن استخدام تقنيات إعادة التشكيل، مثل المصفوفة التكيفية وإعادة التوصيل الديناميكي، يساهم في تحسين كفاءة الأنظمة الشمسية بشكل ملحوظ مقارنة بالطرق التقليدية. كما تبين أن دمج هذه الخوارزميات مع تقنيات **MPPT** يحقق أداءً أفضل في ظروف التظليل الجزئي. توصي الدراسة بضرورة تبني استراتيجيات إعادة التشكيل في تصميم الأنظمة الكهروضوئية لتحقيق استقرار وكفاءة أعلى.

كعمل مستقبلي، يُقترح اختبار هذه الخوارزميات عمليًا على أنظمة حقيقية وربطها مع الشبكات

الكلمات المفتاحية: MPPT، التظليل الجزئي، الخلايا الكهروضوئية، الطاقة الشمسية، إعادة التشكيل.

1. Introduction

Despite being one of the renewable energy sources with the greatest rate of growth, photovoltaic (PV) technology is extremely susceptible to environmental factors. PV modules' output power drastically drops when they are partially obscured by trees, clouds, or adjacent structures. This can result in hot spots and mismatch losses, which can cause long-term system degradation and make maximum power point tracking (MPPT) controllers difficult to utilize (Shams El-Dein, 2012; Serna-Garcés et al., 2016). Only a limited amount of protection against these shading effects is provided by conventional interconnection systems like series-parallel and total cross-tied (Candela et al., 2007; Shams El-Dein, 2012).

http://www.doi.org/10.62341/smay0803

Researchers have suggested reconfiguration methods that dynamically change the electrical connections between PV modules in order to overcome these difficulties. These methods lower power losses and increase overall efficiency by more uniformly spreading irradiance across rows or strings (Buddha, 2011; Romano et al., 2013). A variety of tactics have been investigated, including optimization-based techniques that identify near-optimal layouts for reducing shading losses (El-Dein et al., 2013; Parlak, 2013); adaptive banking, which combines a small reconfigurable array with a fixed array to simplify implementation (Nguyen & Lehman, 2008); and switching matrices and irradiance-equalization methods that continuously rearrange module connections (Romano et al., 2013).

Using MATLAB simulations, this paper offers a comparative analysis of several PV array reconfiguration techniques. To investigate how well dynamic reconfiguration and adaptive banking performed in comparison to traditional interconnection systems, a number of shading scenarios were modeled. Particularly when combined with MPPT algorithms under actual operating conditions, the results provide insights into how these techniques might improve power extraction and system reliability (Candela et al., 2007; Nguyen & Lehman, 2008; Romano et al., 2013; Serna-Garcés et al., 2016).

2. Reconfiguration of solar systems

In photovoltaic systems, clouds, buildings, or trees can shade one or more solar modules. The shaded module's power will soon drop. If this module is linked in series with other non-shaded modules, the shaded module will control the current of all series-connected modules. The darkened module or cell will operate as a load, absorbing the power generated by preceding or subsequent cells. As a result, this module's temperature will rise, triggering the "hot spot" phenomenon and destroying the shaded cell (Shaaban, 2011). Another method for avoiding partial shading is to employ adaptively changeable structures that can be altered depending on the environment.

3. PV Configurations (Interconnection Schemes)

Photovoltaic systems can be configured in four different ways. Each of these setups has unique advantages and downsides. Fig.1 depicts the four schemes: series parallel connection (SP), total cross-tied

http://www.doi.org/10.62341/smay0803

connection (TCT), bridge-linked connection (BL), and honeycomb connection (HC).

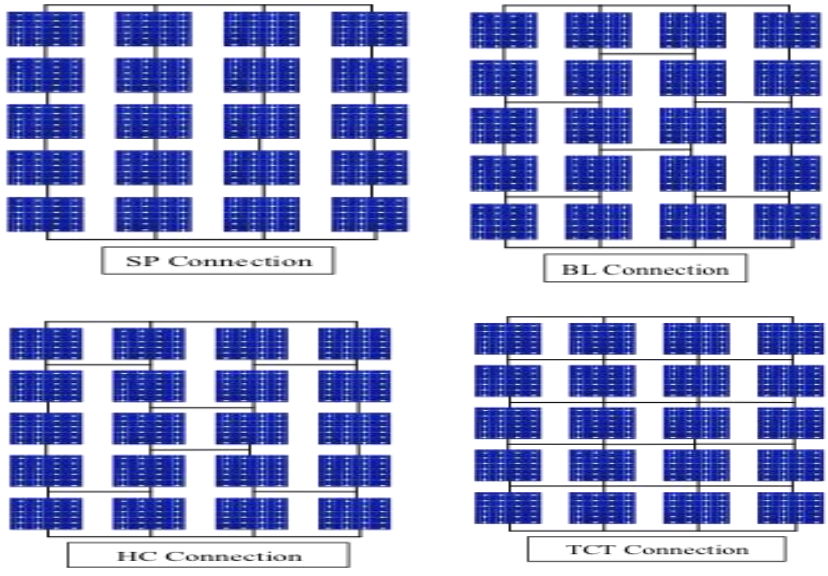

Fig.1. Different connection configurations of solar cells.

The series parallel connection is a parallel connection between items that are connected in series. To ensure that all parallel strings have equal voltages, the number of series elements used to form them must be equal. This connection option is not ideal for systems that receive partial shading. The shaded elements generate less current than their non-shaded counterparts. The elements that create less current will be compelled to disperse some of the energy from the other elements. The total current flow will be reduced, resulting in a power reduction. In the TCT scheme, the connection is represented as a sequence of parallel-connected modules. It has an advantage over the SP method in that the shading effect in one element is applied to all of its parallel colleagues. (Shams El-Dein, 2012).

3.1 Bypassing diode as partial shading solution

Bypass diodes are connected in parallel with a solar cell, panel, or module to provide a free bath for other modules' current during partial shadowing. Fig.2 depicts the connection of a bypass diode in the case of two series modules. If one of the two series modules is shaded, the generated current is reduced. The diode in this situation

http://www.doi.org/10.62341/smay0803

will provide a path to the difference between the string current and the shaded module current (Serna-Garcés et al., 2016).

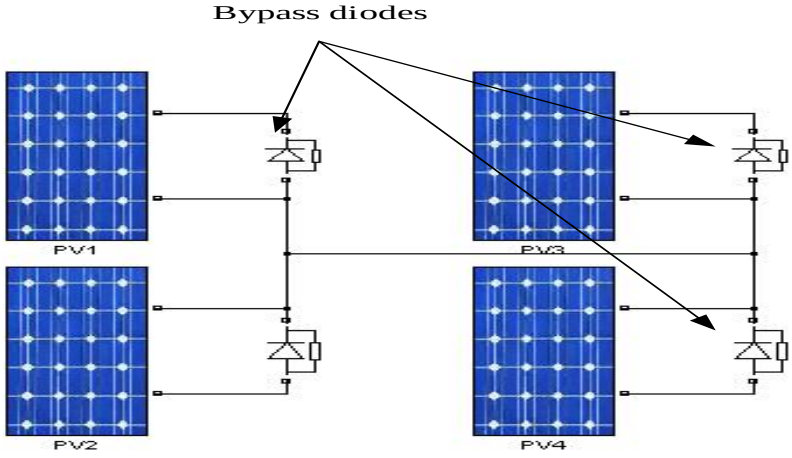

Fig.1. Bypass diodes connection in parallel with solar modules

3.2 Irradiance equalization method

In this method, the modules are reorganised based on the illumination they receive, so that each row of the structure receives the same illumination as the others. The modules or arrays are rearranged using a switching matrix. Fig.3 depicts the concept of irradiance equalisation (Buddha, 2011). Consider having nine modules connected in three series arrays. If the illumination of each module is as indicated in fig. 3.a, the algorithm will attempt to identify another configuration similar to that shown in fig. 3.b. The goal is to make the total irradiance of the rows equal.

This way, the current flows evenly from one row to the next. In the situation of unequal lighting, such as b, the current in the lower row (G=1200) exceeds that in the middle row (G=900). The latter generates higher current than the upper row (G = 600). As a result, the middle row will limit the current in the lower row. Furthermore, the higher row will limit the current in the middle row. The least lighted row will limit the overall current because they are connected in series.

http://www.doi.org/10.62341/smay0803

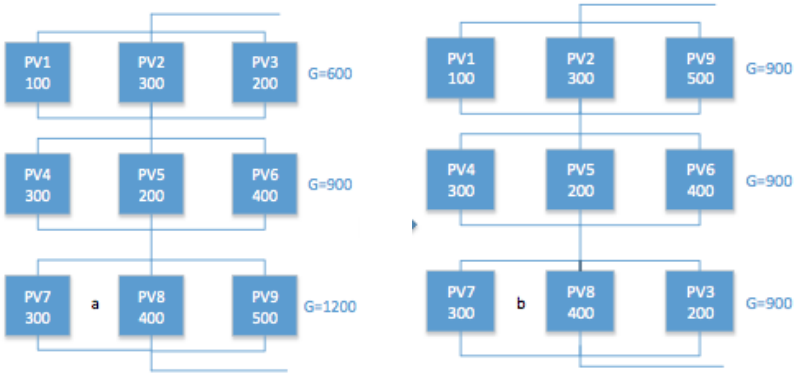

Fig.3 a,b: Irradiance equalization principle

3.3 Dynamic electrical scheme configuration

The parallel connection is widely recognised as the best design for a group of non-uniformly irradiated PV panels. However, this arrangement is practically impractical since it does not meet the maximum current restrictions of the attached power converter (inverter or MPPT) (Romano et al., 2013). It also fails to meet the system's minimum voltage requirement for the power converter. On the other hand, Candela et al. (2007) discovered that connecting non-uniformly irradiated PV modules in series yields the highest power output. The DES design is made up of series connections between parallel-connected modules called "Total Cross Tie TCT". Fig.4 shows the switching matrix, which allows for configuration in a single string of parallel-connected modules.

It is vital to note that this setup is entirely changeable in terms of the number of series modules and parallel arrays. The configuration limits are the power converter's maximum allowable voltage and current. Hence, the reconfiguration method is in charge of finding the maximum number of parallel arrays and series modules (Romano et al., 2013).

The goal is to reorganise the connections of the PV system elements so that the shaded elements are not in series with the non-shaded sections.

Implementing such a strategy for n PV generators requires the use of n*n double pole switches for parallel connections. Furthermore, another single pole switch is used for the series connection of each row in the suggested architecture. Specifically, the system requires n*{n+1} switches to function properly.

http://www.doi.org/10.62341/smay0803

Configuration systems typically use electronic switches (IGBT or MOSFET) or electromagnetic relays (Balato et al., 2015).

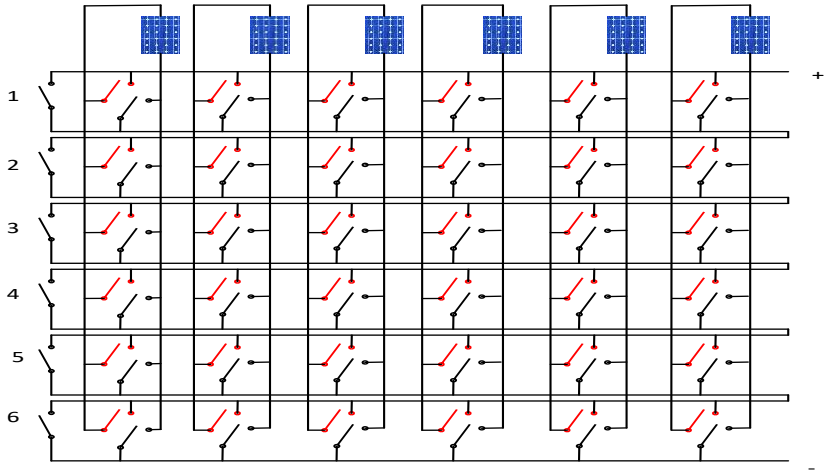

Fig.4.- 6 by 6 switching matrix structure

3.3.1 Reconfiguration algorithm

By reducing the number of series connections between modules with varying levels of radiation, the reconfiguration procedure seeks to optimize the power production from solar generators. There are four primary steps in using the irradiance equalization concept: Initialization: Establish the system's parameters, including permitted rows and parallel connections and voltage and current restrictions.

Data Acquisition: Determine each module's irradiance.

Choose the Best Configuration: Determine the best connection based on limitations and irradiance.

System Reconfiguration: To improve system performance, implement the new configuration (Romano et al., 2013).

3.3.2 Process of finding the best configuration

Finding best configuration is based on a simple search algorithm that employs the acquired (or estimated) irradiation data in its function. The total illumination in a row is defined by:

$$G_j = \sum_{i=1}^{n} G_i \qquad (1)$$

http://www.doi.org/10.62341/smay0803

Where n is the number of elements of the row, j is the row number, G is the illumination. For each configuration, an equalization index is calculated by (Romano et al., 2013):

$$E = \max(G_j) - \min(G_j) \quad ,\forall j$$

(2)

Where j is the index row

This index shows the distribution of illumination over the rows. Whenever the index is minimal, the illumination is better distributed and all rows have equalized illumination according to (Romano et al., 2013).

The procedure starts by initializing the parameters, and then the illumination values of each module are acquired.

3.4 Adaptive reconfiguration (adaptive banking) method

This method was described by Nguyen and Lehman (2008) as a viable reconfiguration method. Instead of making all components of the PV system programmable, it recommends combining one small reconfigurable bank of PV arrays with a bigger bank of non-reconfigurable arrays. A switching matrix connects the small and large banks. This system minimizes the number of switches used as well as the algorithm's scanning time. Fig.5 depicts the array connections for the large (fixed) part of the construction. The reconfigurable half is made up of m free solar cells that can be linked in parallel to any module in the fixed part (Karakose et al., 2014; Velasco et al., 2014).

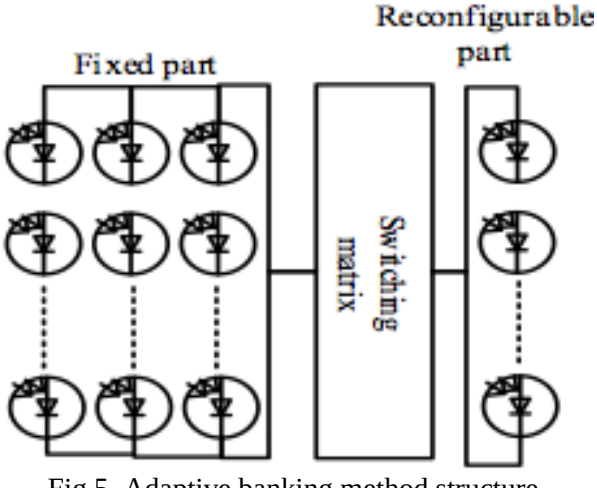

Fig.5. Adaptive banking method structure

http://www.doi.org/10.62341/smay0803

3.4.1 Algorithm 1

The shaded module is identified by comparing its voltage to the average voltage of the remaining modules. Once a shaded module is identified, one adaptive array is linked to it. In the initial setup, the adaptive arrays were randomly coupled to the fixed modules. (Nguyen and Lehman, 2008).

The reconfiguration method involves disconnecting all adaptive bank switches, measuring adaptive array voltages, and sorting them in decreasing order (V1>V2>…>Vm). The voltages of the fixed part modules are also organised in ascending order, low to high. The switching matrix is triggered again, and the greatest open circuit voltage of the adaptive bank arrays is linked to the lowest fixed module voltage (the most shaded).

3.4.2 Algorithm 2

This algorithm connects the entire system and measures the voltages of each module. The adaptive array's open circuit voltage and cell temperature are also measured and utilised to estimate the array's currents. According to Nguyen and Lehman (2008), the photo-generated current of each adaptive bank array is:

$$I_{Aj} = \frac{V_{ocAj}}{R_{sh}} + I_s \left[e^{\frac{qV_{ocAj}}{akT}} - 1 \right] \tag{3}$$

Where:

I is the photo-generated current, Is is the dark saturation current , V is thermal voltage (V) for the module, q is the charge of electron, k is Boltzmann's constant, R_{Sh} is the shunt resistance T is the temperature, a is the ideality factor of the diode between 1 and 2.

$$I_{Fj} = I_{out} + nI_s \left[e^{\frac{q(V_j + I_{out}R_{sM}}{akT}} - 1 \right] + \left[\frac{V_j + I_{out}R_{sM}}{R_{shM}} \right] \tag{4}$$

Where:

Rs is the series resistance

4. Results and discussions

The following system model was created to demonstrate the impacts of partial shadowing on various topologies of PV systems using Matlab/Simulink. The parameters of the simulated system are shown in Table.1. The system will be simulated using 24 PV panels. Fig.6 illustrates how the panels are originally joined. Various

http://www.doi.org/10.62341/smay0803

connection topologies were used on the PV panels. Table 2 shows the irradiation levels and shading of the panels for each case. In the first example, the simulation will take into account a fully irradiated system with an irradiation of 1000w/m2. The remaining instances will address various partial-shading scenarios. The goal is to investigate how shade affects the various connection topologies of PV systems.

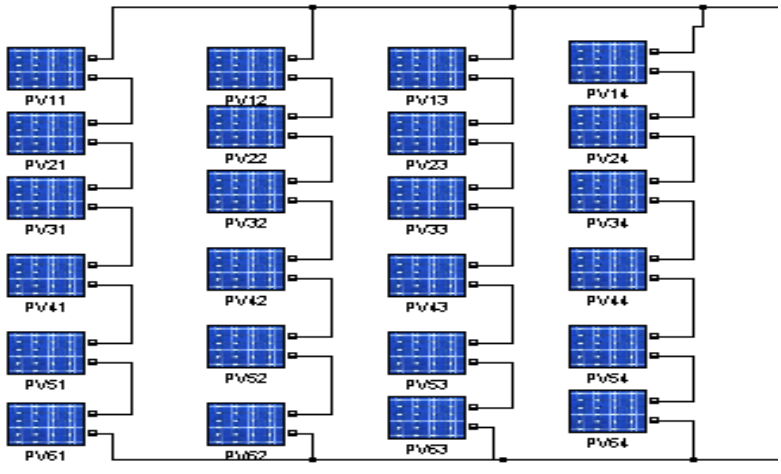

Fig.6. PV panels used in the simulation

Table.1. Parameters of the PV panels

Voc	64.2 v	Imax. Power	5.5 A	ki	0.0617
Isc	5.87 A	Max. Power	300W	kv	-0.272
Series cells	96	Rp	269.5 Ω	a	0.945
Vmax. Power	54.7 v	Rsh	0.37 Ω	No. Panels	24

Table.2. Different shading parameters of the simulated system

Case 1

1000	1000	1000	1000
1000	1000	1000	1000
1000	1000	1000	1000
1000	1000	1000	1000
1000	1000	1000	1000
1000	1000	1000	1000

Case 2

500	1000	1000	1000
500	1000	1000	1000
500	1000	1000	1000
500	1000	1000	1000
500	1000	1000	1000
500	1000	1000	1000

Case 3

500	500	500	500
1000	1000	1000	1000
1000	1000	1000	1000
1000	1000	1000	1000
1000	1000	1000	1000
1000	1000	1000	1000

Case 4

1000	1000	1000	1000
1000	1000	1000	1000
500	1000	1000	1000
500	500	1000	1000
500	500	500	1000
500	500	500	500

http://www.doi.org/10.62341/smay0803

4.1 Equally distributed irradiation, case 1

In this scenario, the whole matrix of PV panels will receive the same irradiation levels.

All the topologies have given the same results with the system at its maximum efficiency as shown in fig.7. The maximum power value was approximately 7.2kW.

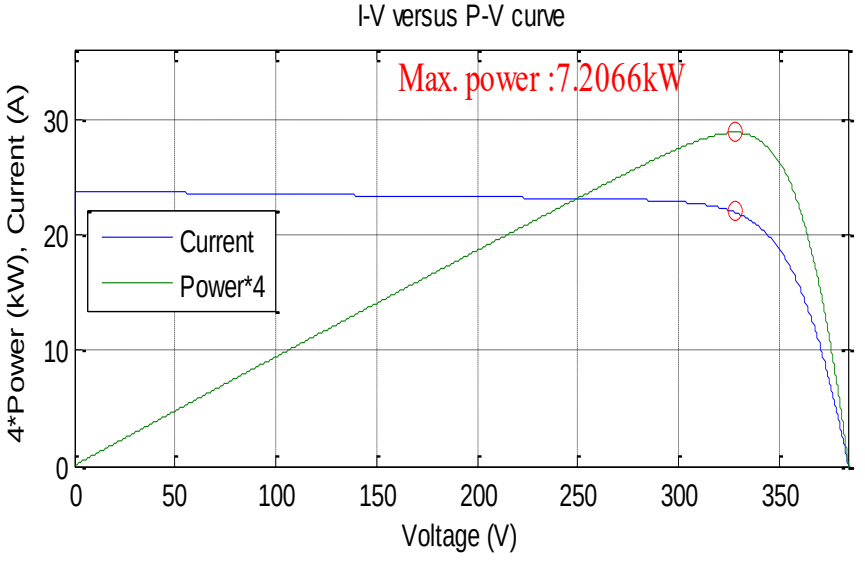

Fig .7. The performance of the solar system under no partial shading conditions

4.2 Partial shading of one column of the matrix, case 2

Figs 8–10 show the results. These figures illustrate that darkening one column (of series elements) reduces generated power in all topologies.

It is worth noting that the shading was consistent across the entire column. Six series elements were partially irradiated, resulting in an approximately 900W reduction in generated power. The generated power has been lowered from 7206W to 6254W across all topologies. This means that partial shading in one column has no effect on non-shaded elements.

http://www.doi.org/10.62341/smay0803

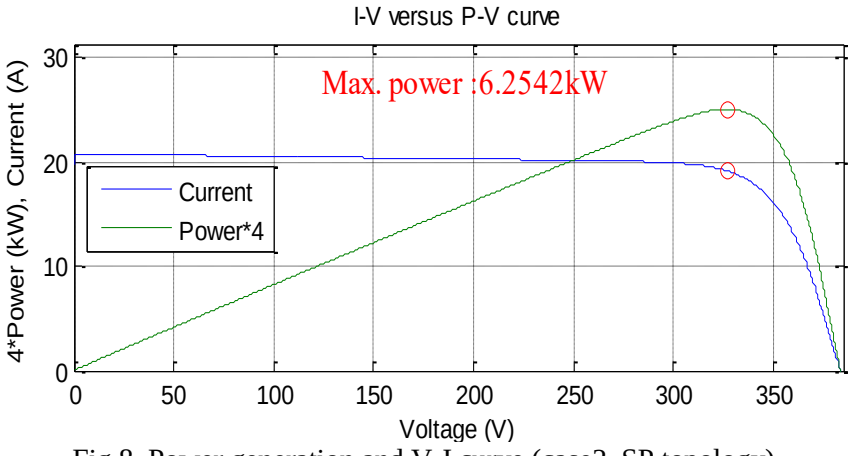

Fig.8. Power generation and V-I curve (case2, SP topology)

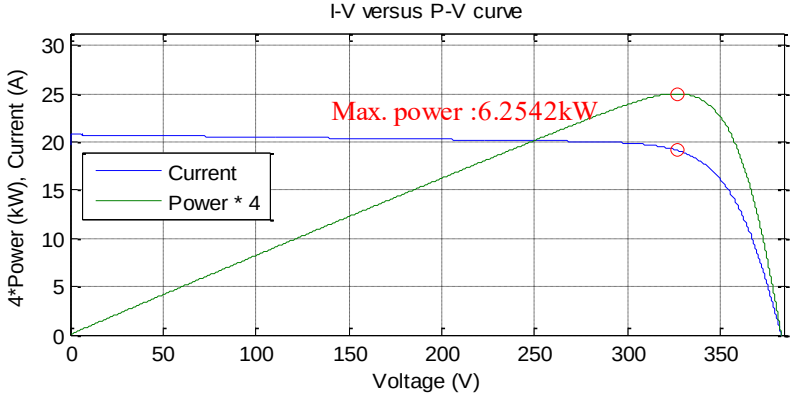

Fig .9. Power generation and V-I curve (case2, TCT topology)

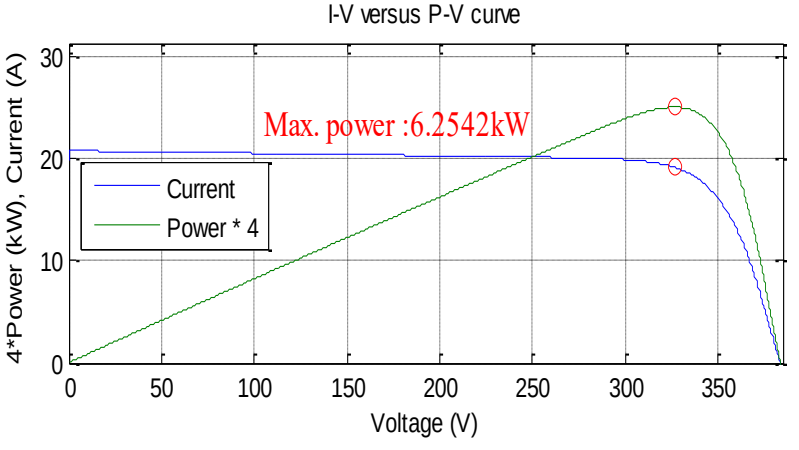

Fig.10. Power generation and V-I curve (case2, parallel diode topology)

http://www.doi.org/10.62341/smay0803

4.3 Partial shading of horizontal line of the PV matrix, case 3

The shaded line was lighted at 500W/m^2. Fig.11 depicts the P-V and I-V curves of a system coupled in SP topology. Figure 12 depicts the findings utilising TCT topology. These two statistics indicate that illuminating one line lowered the power to half of its full capacity. While the actual power reduction should be 600W, the shaded elements were connected in series, dissipating approximately 3kW in the shaded panels. Fig. 13 depicts the usage of parallel diodes to mitigate the effects of partial shading on series-connected PV generators. The generated power has decreased from 7200W to 5975W since all shaded elements were cancelled, and some power dissipation occurs owing to the use of diodes. 1225W were lost from the system as an effect instead of 600W.

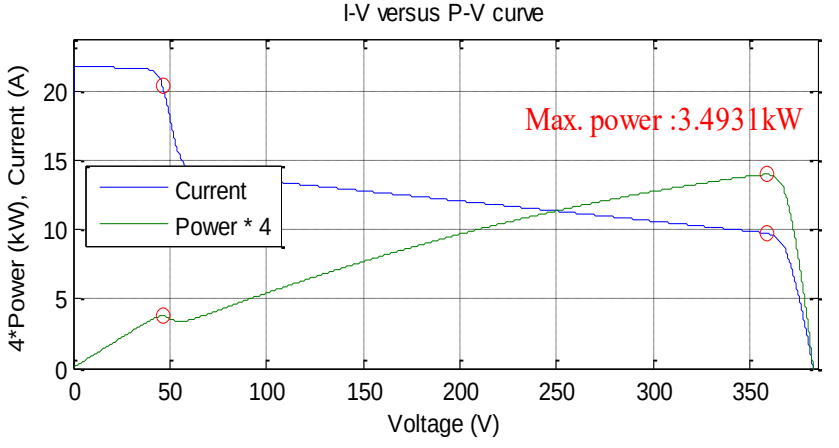

Fig.11. Power generation and V-I curve (case3, SP topology)

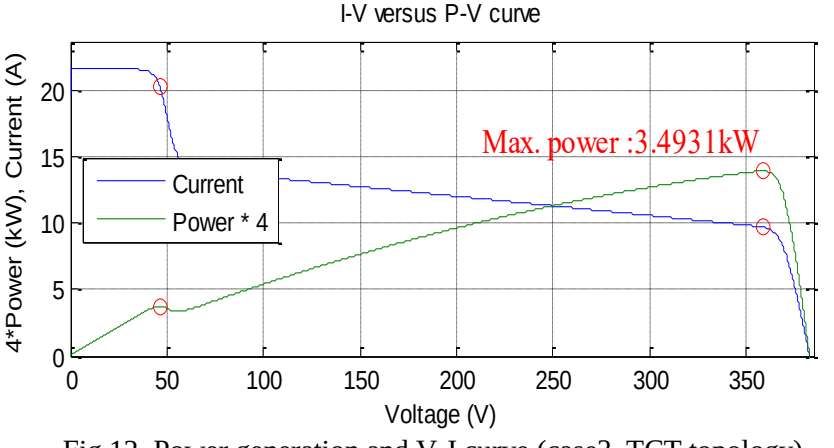

Fig.12. Power generation and V-I curve (case3, TCT topology)

http://www.doi.org/10.62341/smay0803

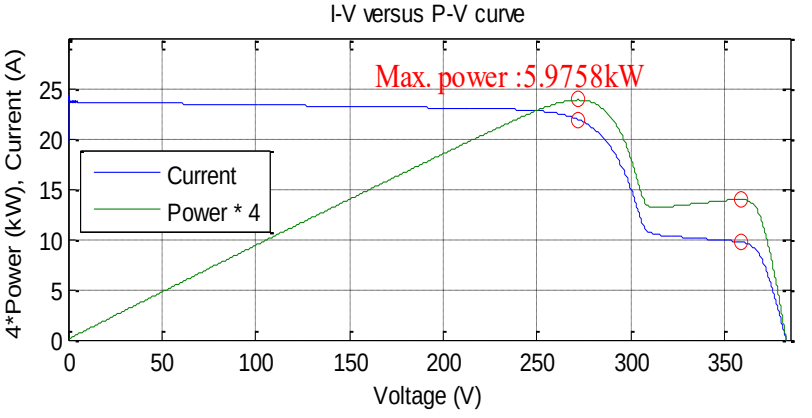

Fig.13. Power generation and V-I curve (case 3, parallel diode topology)

4.4 Partial shading of triangular group of elements, case 4

In this situation, the triangular group of items with ten elements was darkened. This group received 500W/ m^2 irradiation. A reduction of 1500W in individual generated electricity was projected. However, simulation results indicate that the drop in generated power is greater. Figures 14, 15, and 16 demonstrate that the generated power was around half of the nominal power. SP topology produced the poorest results, with a power dissipation of 3750W. In this topology, the columns with shaded elements create electricity as if the entire column were shaded. The TCT topology produced a somewhat better outcome, as illustrated in Figure 14. However, the power losses remain substantial. The parallel diode topology had the best performance, with around 3790W.

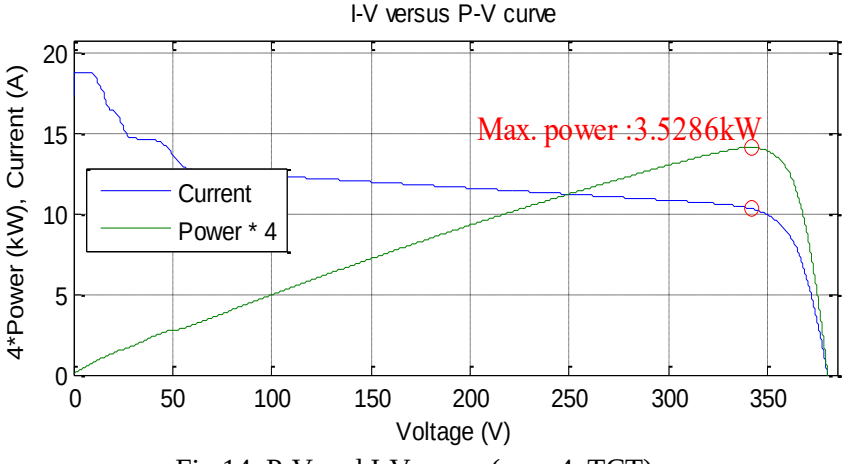

Fig.14. P-V and I-V curve (case 4, TCT).

http://www.doi.org/10.62341/smay0803

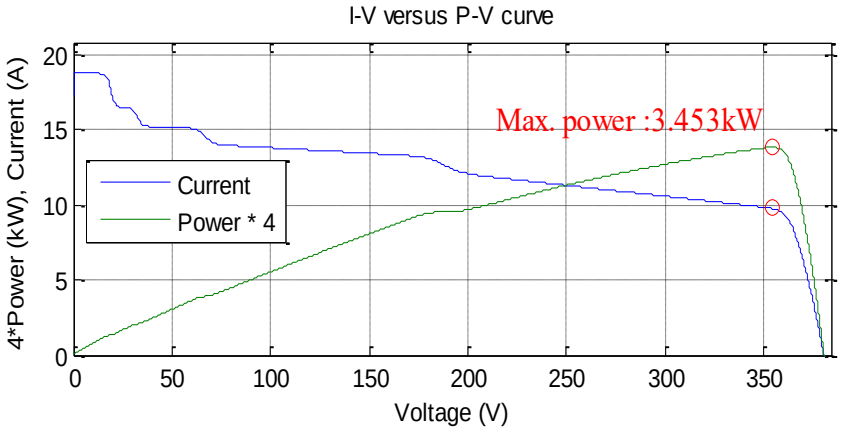

Fig.15. P-V and I-V curve (case 4, SP)

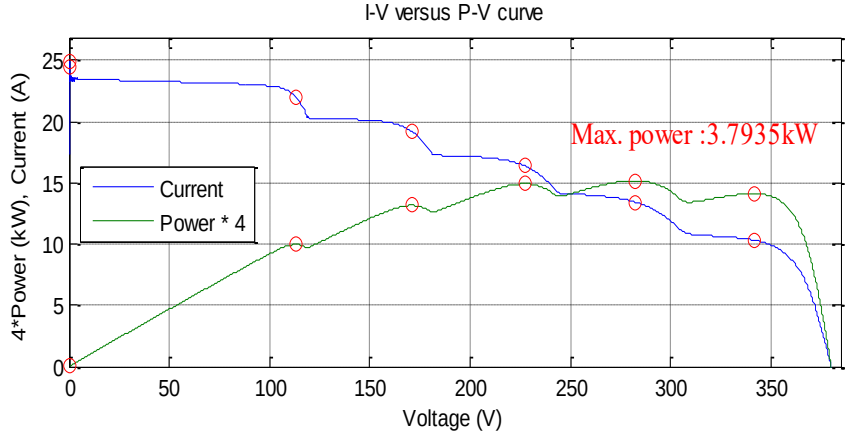

Fig.16. P-V and I-V curve (case 4, parallel diodes)

4.5 Partial shading of one column of the matrix, case 2

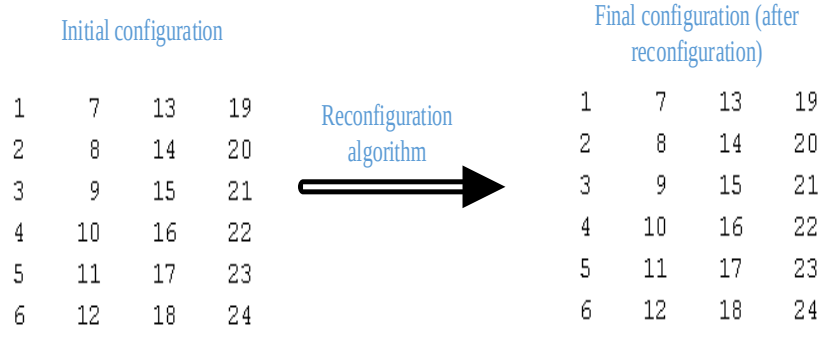

Fig.17. Panel matrix order before and after reconfiguration, case 2

http://www.doi.org/10.62341/smay0803

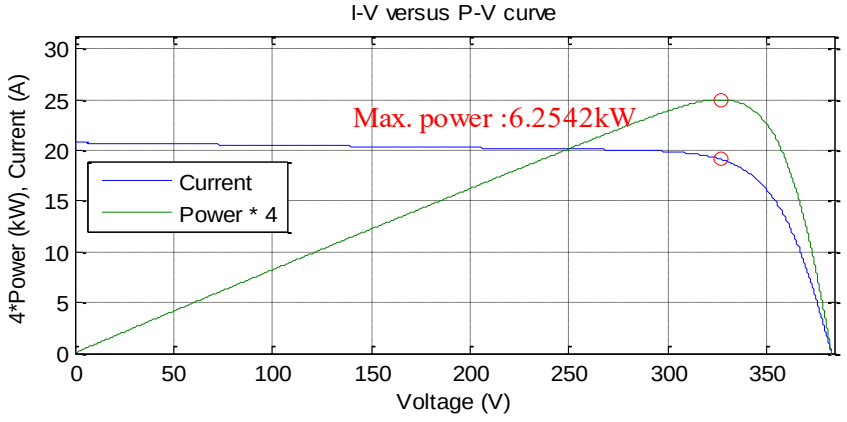

Fig.18. Results of the system after reconfiguration, case 2

4.6 Partial shading of horizontal line of the PV matrix, case 3

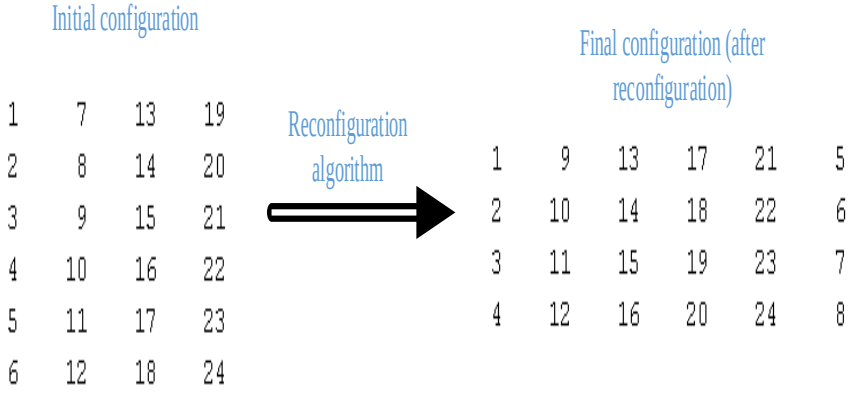

Fig.19. Panel matrix order before and after reconfiguration, case 3

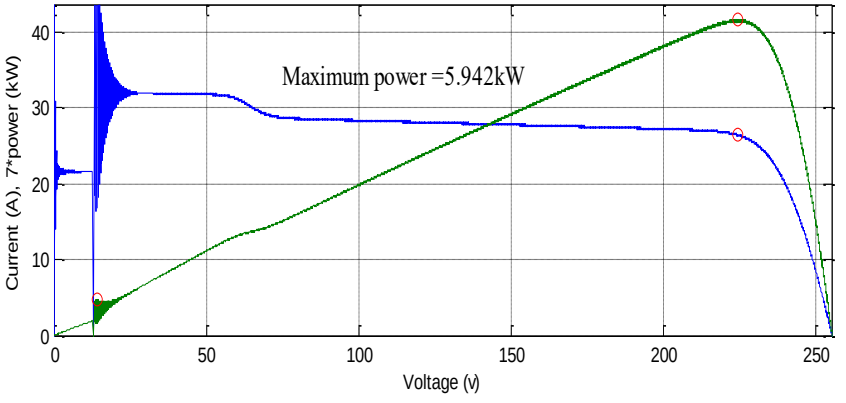

Fig.20. Results of the system after reconfiguration, case 3

http://www.doi.org/10.62341/smay0803

4.7 Partial shading of triangular group of elements, case 4

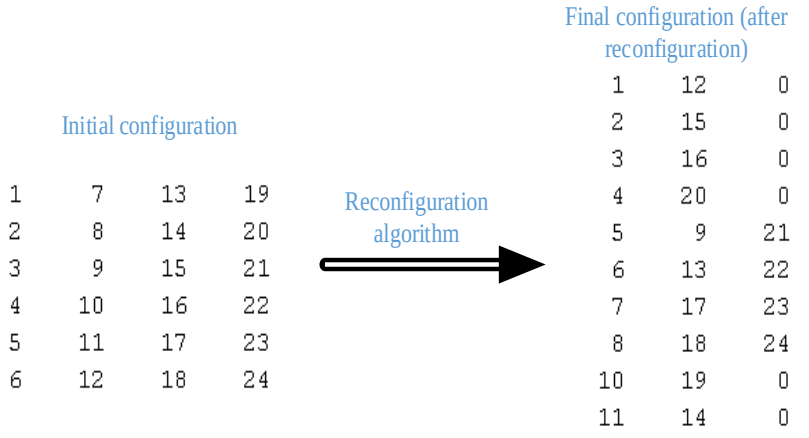

Fig.21. Panel matrix order before and after reconfiguration, case 4

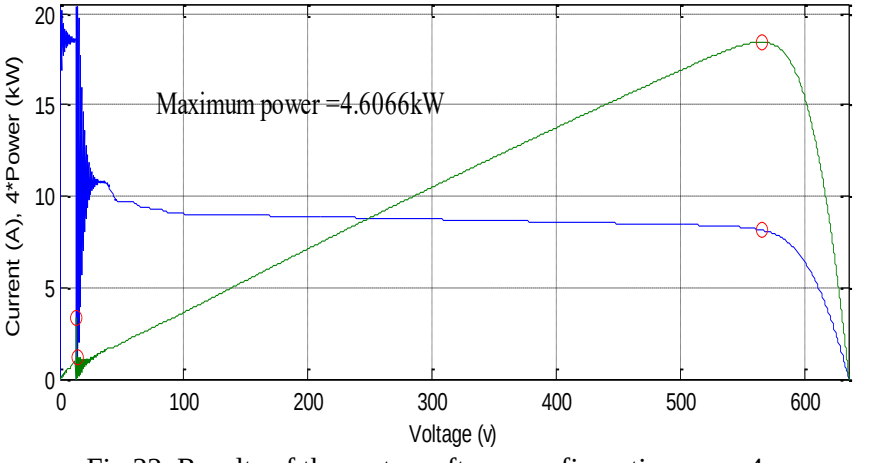

Fig.22. Results of the system after reconfiguration, case 4

As Figs 16-22 show, the reconfiguration process rearranges the connections between the elements of the matrix. The elements of each row in the reconfigured matrix are connected in parallel.

4.8 Adaptive bank reconfiguration

One column of our 6*4 solar array elements was employed as an adaptive bank, while the other three columns were regarded fixed banks. Fig.23 depicts the SIMULINK model of the adaptive bank. The graphic depicts the switching matrix used to connect the

http://www.doi.org/10.62341/smay0803

adaptive bank elements to the fixed bank elements. The switching matrix comprises of 36 switches that govern the link between the adaptive bank elements and the fixed elements.
The switching matrix comprises of 36 switches that govern the link between the adaptive bank elements and the fixed elements. Each of the six adaptable panels can be connected to one row of fixed panels at a time using a single switch. The switching matrix is divided into six blocs, each of which consists of six double pole switches. Figs 23 and 24 depict the structure of the bloc, with each bloc capable of connecting one fixed row to any of the six adaptable elements.

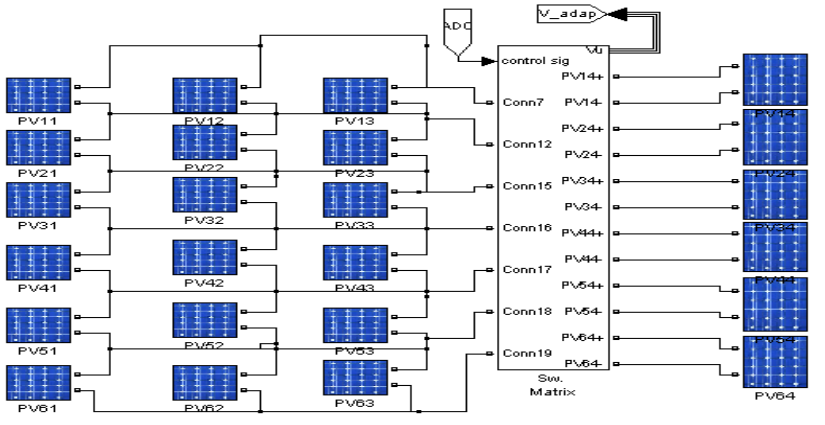

Fig .23. Simulation model of the adaptive bank

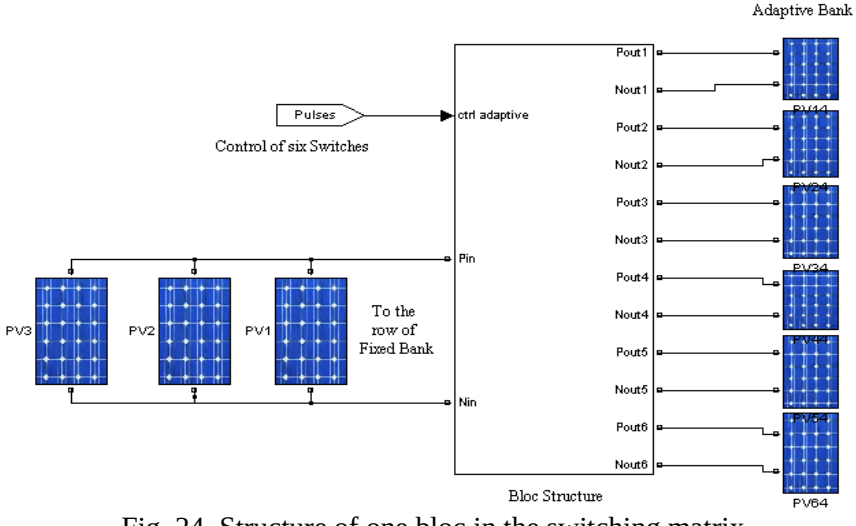

Fig .24. Structure of one bloc in the switching matrix

4.8.1 First configuration

The table 3 depicts the illumination strategy for the system arrays in this configuration. Figs 25 and 26 show the system power and

http://www.doi.org/10.62341/smay0803

current results before adaptive reconfiguration. The figures illustrate that the maximum achievable power in this example is 3.47kW, with three distinct maximum power spots on the power curve. The occurrence of several maximum power points has an impact on the functionality of MPPT.

Table.3. Irradiation scheme of the first configuration

500	500	500	500
500	500	500	1000
1000	1000	1000	1000
1000	1000	1000	1000
1000	1000	1000	1000
1000	1000	1000	1000

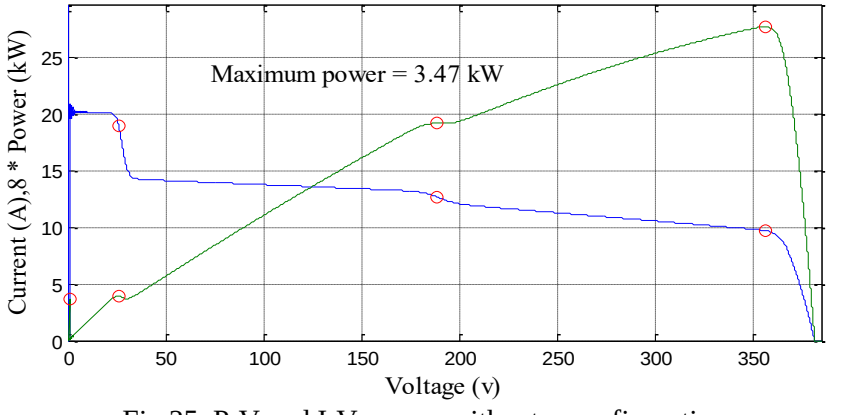

Fig.25. P-V and I-V curves without reconfiguration

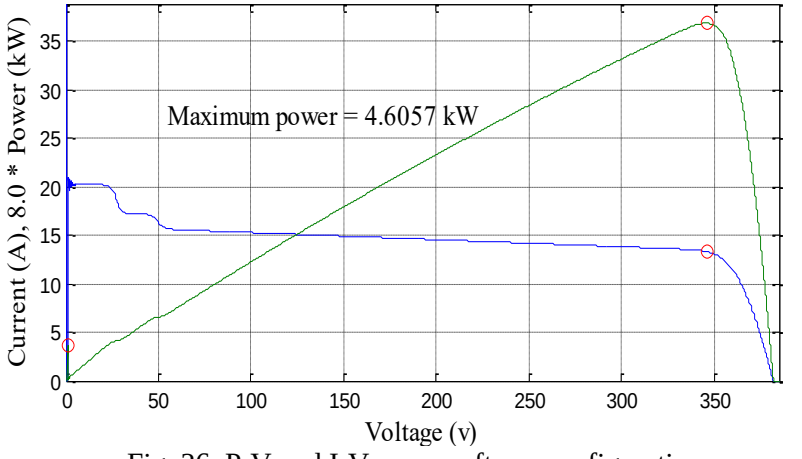

Fig .26. P-V and I-V curves after reconfiguration

http://www.doi.org/10.62341/smay0803

Multiple maximum points may cause the MPPT device to select a local maximum point incorrectly and interpret it as the true maximum power point. As a result, the system may produce less power than it is capable of producing in the same circumstances. The system's generated power following the implementation of the adaptive reconfiguration technique is shown in Fig.26. As we can see from the initial glance, the power has increased to 4.6 kW from 3.47 kW prior to the reconfiguration. One maximum point on the P-V curve indicates improved MPPT device performance.

4.8.2 Second configuration

Fig.27 depicts the usually generated power from the system in the absence of any reconfiguration algorithms. The chart demonstrates that the system can extract a maximum of 4.05kW of power.

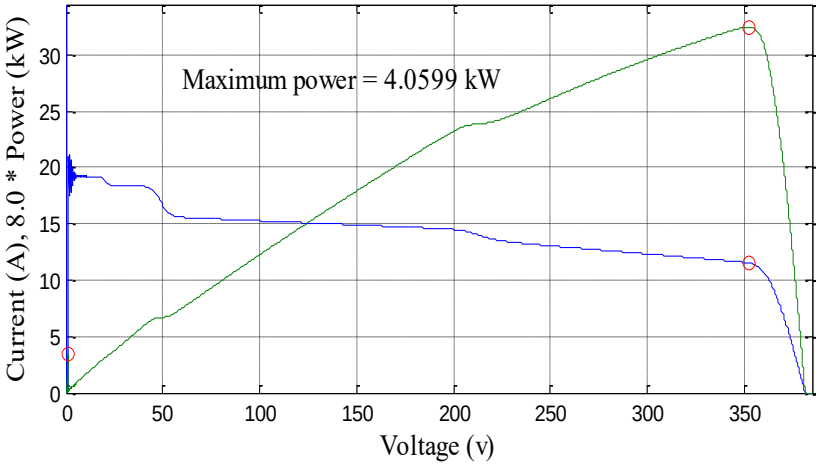

Fig .27. Power and current curves in the second scheme (without reconfiguration)

Table 4 displays the irradiation technique in this arrangement.

Table.4. Irradiation scheme of the second configuration

300	500	1000	500
500	1000	1000	1000
500	1000	1000	200
500	1000	1000	1000
500	1000	1000	1000
1000	1000	1000	1000

http://www.doi.org/10.62341/smay0803

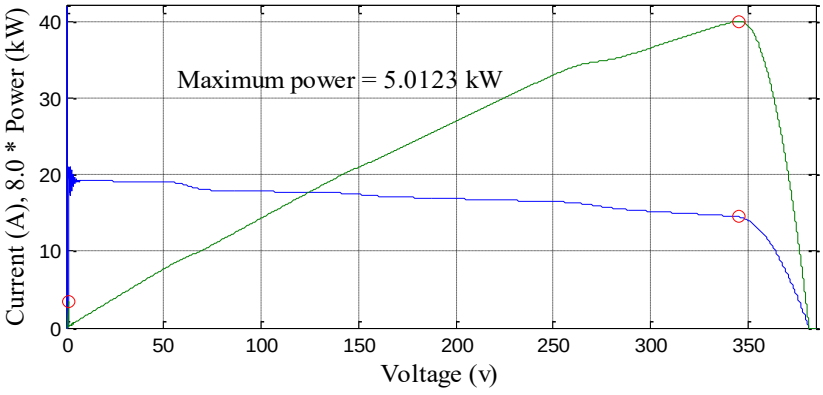

Fig.28. Power and current of second scheme after using reconfiguration

Under the same irradiation conditions, the power has been increased from 4.05 to 5.01kW as shown in fig. 28 following the reconfiguration algorithm's application. In this instance, the MPP tracker functions are unaffected by the two curves' single maximum power point.

4.8.3 Third configuration

In this configuration, the solar array was irradiated in accordance with table 5. The triangular region of the system was partially darkened to investigate its effect on the system. The table displays the different irradiation levels used. Fig.29 shows the power and current curves as a function of PV voltage. The greatest power that can be extracted from the system under these conditions without reconfiguration is 4.12kW. However, using the adaptive bank-based reconfiguration approach resulted in a maximum extracted power of 5.21kW.

Data in Fig.30 demonstrate that, the power curve seems to be smooth when there is only one maximum power point. The reconfiguration method significantly improved the system's efficiency under partial shade situations.

Table.5. the irradiation of the solar array in its third configuration.

1000	1000	1000	1000
1000	1000	1000	600
500	400	1000	1000
700	200	1000	1000
850	500	600	400
1000	1000	300	300

http://www.doi.org/10.62341/smay0803

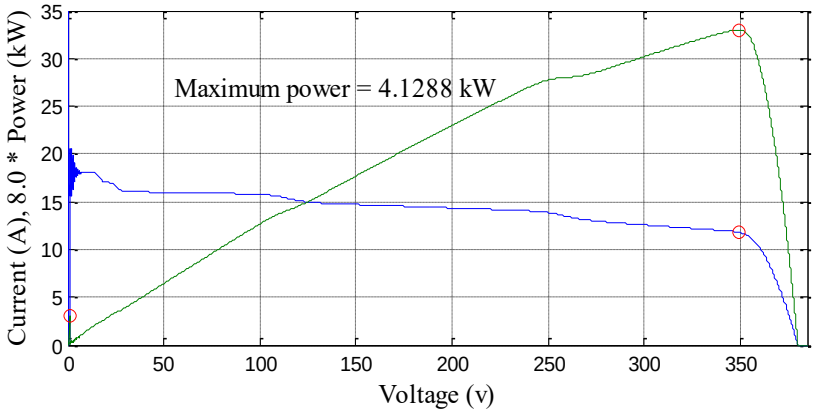

Fig.29. P-V and I-V curves without reconfiguration

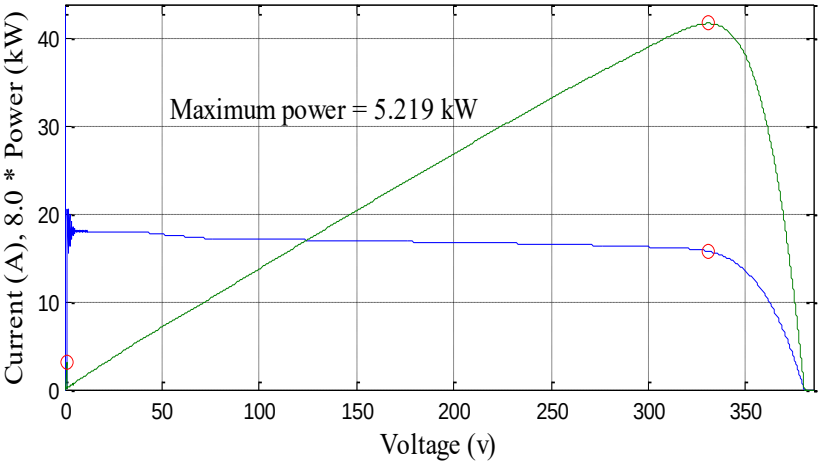

Fig.30. P-V and I-V curves after reconfiguration

5. Conclusions

The problem of partial shade in solar systems has been studied in this work, and several reconfiguration techniques have been assessed in an effort to lessen its adverse effects. According to simulation results, mismatch losses under non-uniform irradiance circumstances cannot be adequately addressed by traditional topologies like series-parallel and total cross-tied. On the other hand, sophisticated techniques like adaptive banking, dynamic reconfiguration, and irradiance equalization greatly enhanced power extraction and system stability.

The results validate that the use of reconfiguration algorithms improves MPPT controller performance by lowering the frequency of numerous power peaks and increasing overall efficiency. Of the

http://www.doi.org/10.62341/smay0803

techniques examined, dynamic electrical schemes provided significant gains for larger shaded areas, while adaptive reconfiguration worked best for confined shading situations.
Future work should focus on experimental validation of these algorithms using real PV systems, as well as exploring their integration with microgrids and smart control frameworks to ensure reliable operation in diverse environments. By adopting these strategies, PV system designers and operators can achieve higher energy yields, improved reliability, and greater sustainability in solar energy applications.

References

Buddha, S. T. (2011). *Topology Reconfiguration To Improve The Photovoltaic (PV) Array Performance*. Arizona State University.

Candela, R., Dio, V. d., Sanseverino, E. R., & Romano, P. (2007). Reconfiguration Techniques of Partial Shaded PV Systems for the Maximization of Electrical Energy Production. *2007 International Conference on Clean Electrical Power* (pp. 716-719). IEEE. doi:10.1109/ICCEP.2007.384290.

Cheng, Z., Pang, Z., Liu, Y., & Xue, P. (2010). An adaptive solar photovoltaic array reconfiguration method based on fuzzy control. *8th World Congress on Intelligent Control and Automation (WCICA)* (pp. 176-181). Jinan: IEEE. doi:10.1109/WCICA.2010.5553911.

El-Dein, M. Z., Kazerani, M., & Salama, M. M. (2013). Optimal Photovoltaic Array Reconfiguration to Reduce Partial Shading Losses. *IEEE Transactions on Sustainable Energy*, 4(1), 145-153. doi:10.1109/TSTE.2012.2208128.

Guillermo, V.-Q., Francisco, G.-G., Robert, P.-L., Manuel, R.-L., & Alfonso, C.-R. (2009). Electrical PV Array Reconfiguration Strategy for Energy Extraction Improvement in Grid-Connected PV Systems. *IEEE Transactions on Industrial Electronics*, 56(11), 4319-4331. doi:10.1109/TIE.2009.2024664.

Karakose, M., et al. (2014). An Intelligent Reconfiguration Approach Based on Fuzzy Partitioning in PV Arrays. IEEE.

http://www.doi.org/10.62341/smay0803

Karaköse, M., Murat, K., Akın, E., & Parlak, K. S. (2014). A New Efficient Reconfiguration Approach Based on Genetic Algorithm in PV Systems. *IEEE 23rd International Symposium on Industrial Electronics* (pp. 23-28). IEEE.

Nguyen, D., & Lehman, B. (2008). A Reconfigurable Solar Photovoltaic Array Under Shadow Conditions. *IEEE* (pp. 980-986). Northeastern University, Boston.

Nguyen, D., & Lehman, B. (2008). An Adaptive Solar Photovoltaic Array Using Model-Based Reconfiguration Algorithm. *IEEE Transactions on Industrial Electronics*, 55(7), 2644-2654. doi:10.1109/TIE.2008.924169.

Parlak, K. Ş. (2013). A New reconfiguration method for PV array system. *Industrial Electronics Society, IECON 2013 - 39th Annual Conference of the IEEE* (pp. 1478 - 1483). Vienna: IEEE. doi:10.1109/IECON.2013.6699351.

Romano, P., Candela, R., Cardinale, M., Vigni, V. L., Musso, D., & Sanseverino, E. R. (2013). Optimization of Photovoltaic Energy Production through an Efficient Switching Matrix. *Journal of Sustainable Development of Energy, Water and Environment Systems*, 1(3), 227-236. doi:10.13044/j.sdewes.2013.01.0017.

Serna-Garcés, S. I., Bastidas-Rodríguez, J. D., & Ramos-Paja, C. A. (2016, February 9). Reconfiguration of Urban Photovoltaic Arrays Using Commercial Devices. *Energies*, pp. 1-23.

Shaaban, M. A. (2011). *Adaptive Photovoltaic configurations for Decreasing the Electrical Mismatching losses*, MSc. University of Nebraska-Lincoln.

Shams El-Dein, M. Z. (2012). *Novel Designs for Photovoltaic Arrays to Reduce Partial Shading Losses and to Ease Series Arc Fault Detection*, PhD. University of Waterloo.

Solar Micro Inverter, Enphase. (2016, March 17). Retrieved from https://enphase.com/en-us